PSEUDO DYNAMIC TESTING, PERFORMANCE ASSESSMENT, AND MODELING OF DEFICIENT REINFORCED CONCRETE FRAMES

W. Lin[1], H. Sucuoğlu[2], and B. Binici[3]

[1] *Graduate Student, Erasmus Mundus MEEES Program, Middle East Technical University, Ankara*
Email: wesley.lin@empireds.com
[2] *Prof. Dr., Department of Civil Engineering, Middle East Technical University, Ankara*
Email: sucuoglu@metu.edu.tr
[3] *Prof. Dr., Department of Civil Engineering, Middle East Technical University, Ankara*
Email: binici@metu.edu.tr

ABSTRACT:

A pair of ½ scale 3-story, 3-bay concrete bare frames were tested by the pseudo dynamic (PsD) testing procedure. Both frames represent common deficiencies of non-seismic construction. Continuous column reinforcement in one specimen and insufficient lap splices at the bottom ends of columns in the other specimen was the only difference. Measured seismic performance of both frames was assessed by using the rotation and strain based acceptance criteria of two different seismic codes. Dynamic responses of both frames were also predicted by employing nonlinear frame models. Analytical models of deficient frames were capable of predicting global deformation response, but failed to predict local deformations. Prediction of local deformations in deficient frames can only be improved if joint deformations and hysteretic degradation in member properties are considered directly in the analytical models.

KEYWORDS: Deficient Frames, Lap Splices, Pseudo Dynamic Testing, Performance Assessment, Modeling

1. INTRODUCTION

Performance evaluation of deficient buildings has become a major concern in seismic prone regions due to significant economic and human losses caused by their poor performance during earthquakes. The most common deficiencies in buildings constructed before the 1980's in Turkey and her neighboring countries are non-seismic detailing in structural members and joint regions, low material strengths and use of plain reinforcement. Another prominent deficiency were in the column lap splices which were designed for compression only, leading to insufficient development lengths in tension.

The effect of lap splice deficiencies on seismic response has mostly been examined in the literature via individual column tests. There are a limited number of frame tests investigating the behavior of columns with insufficient splice lengths. However, frame tests with such deficiencies tested under realistic earthquake ground motion demands are scarce.

The first objective of the presented study is to provide data on the seismic performance of deficient frames measured under realistic ground motion demands. Two ½ scale 3-story, 3-bay deficient concrete bare frames were tested by the pseudo dynamic (PsD) testing procedure under three subsequent earthquake ground motions representing different intensity levels. Both frames were constructed with low strength concrete, plain reinforcing bars and non-seismic detailing. The main difference was in the column lap splices. One specimen had continuous column reinforcement whereas the other one had insufficient lap splices at the bottom ends of columns. Splice lengths were 25% shorter than that required by the design codes.

Performance assessment of existing concrete buildings has been a major concern during the last two decades in earthquake prone countries. ASCE/SEI 41-06, Eurocode 8-3 and the Turkish Earthquake Code (TEC)

are the published codes and guidelines for regulating seismic performance evaluation of existing buildings in different parts of the World. ASCE/SEI 41 and Eurocode 8-3 suggest performance limits based on plastic end rotations whereas TEC employs strain based performance limits for concrete members. The second objective of this study is to test the validity of deformation based performance assessment criteria by comparing the member performance ratings of ASCE/SEI 41 and TEC with those obtained from experimental observations. The effect of lap splices on seismic performance assessment is given special emphasis.

Analytical prediction of experimental inelastic dynamic frame response is a basic challenge in earthquake engineering. Rigorous nonlinear analytical models have been prepared in this study for both test frames, and the analytical and experimental responses are compared in terms of both the global and local response parameters. The objective of this final task is to evaluate the success of inelastic dynamic frame models in predicting the seismic response of deficient concrete frames.

2. TEST SPECIMENS

The interior bay frame (**Figure 1**, gridline 3) was selected as the test specimen. The column dimensions were 400x300 mm with 1.33% longitudinal reinforcement ratio. The beam dimensions were 300x350 mm, which were uniform in all spans. Test specimen dimensions were ½ of the prototype frame member sizes, as shown in **Figure 2**, along with the notation for the beams and columns.

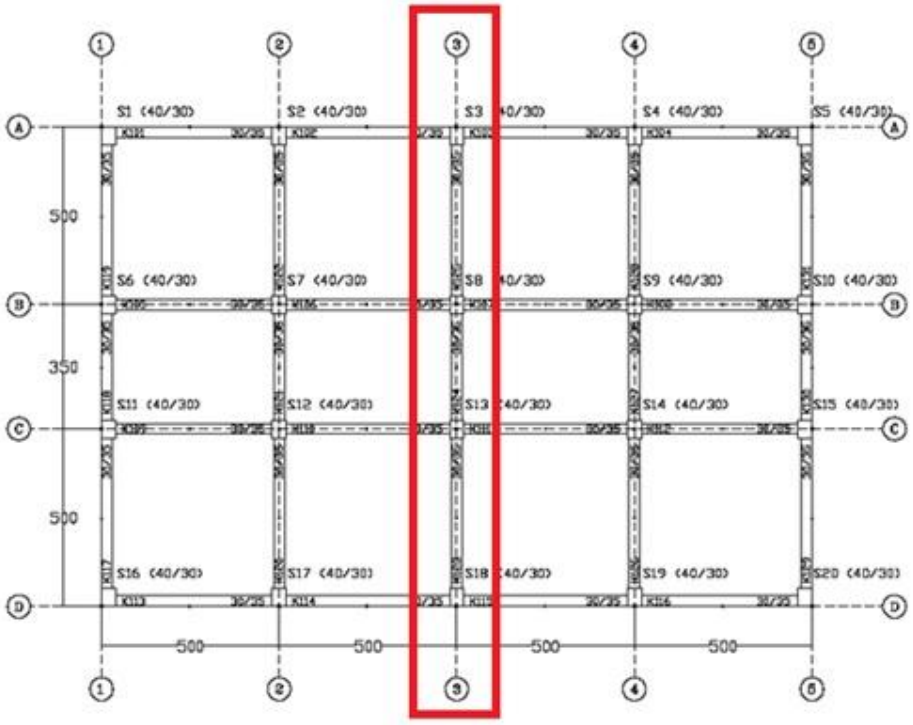

Figure 1. Plan view of prototype building and test frame

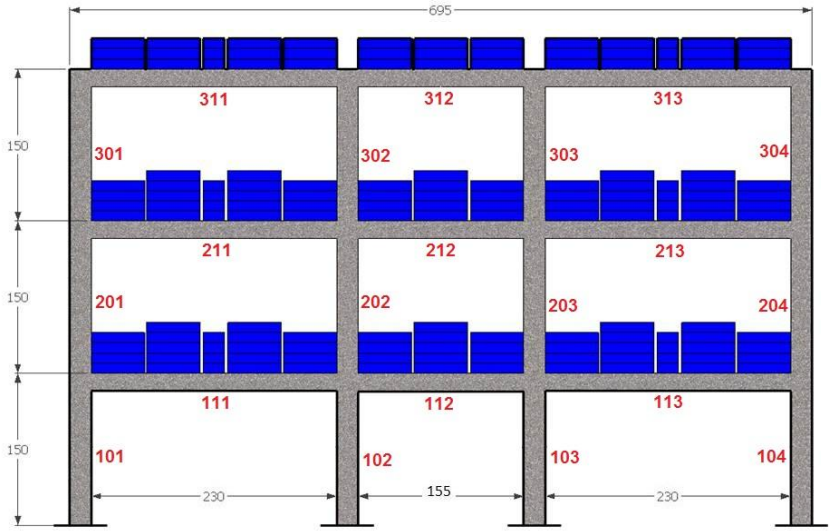

Figure 2. Elevation view of the test specimens

The average uniaxial compressive strength of concrete used for Specimen #1 (SP1) was 11.9 MPa and for specimen #2 (SP2) was 14.0 MPa. All reinforcement were made from plain bars. The yield strengths of column longitudinal reinforcement, beam longitudinal reinforcement and transverse reinforcement steel were 320 MPa, 355 MPa and 240 MPa, respectively, as determined from material tests. SP1 had continuous bars throughout the beams and columns whereas SP2 only had continuous bars throughout the beams. Longitudinal reinforcement at the column bases of SP2 had lap splices with 75% of the splice lengths required by the Turkish Earthquake Code (40 bar diameters for plain bars). Therefore 25% lap splice deficiency is introduced at the column bases of SP2.

All beams have sufficient flexural and shear capacities under gravity loads. Beams are stronger than the columns around the interior joints. The shear capacity of the beams and columns are larger than the shear force at their flexural capacity. Hence flexural response is assured in all frame members. Gravity loads are taken as 4 kN/m^2 in addition to self weight on each floor (**Figure 1**), corresponding to a total line load of 15.7 kN/m along the beams. They were applied through the use of steel blocks, as shown in **Figure 2**. The corresponding axial load ratios of exterior and interior columns at the 1st story are 0.13 and 0.23 for SP1 and 0.11 and 0.20 for SP2, respectively.

3. PSEUDO DYNAMIC TESTING

Pseudo-dynamic testing is a hybrid earthquake simulation technique which combines numerical modeling of the structural properties with a physical test run in parallel with computations. This testing method was developed as an alternative to shake table testing. Through pseudo-dynamic testing, it is possible to accurately simulate large-scale structural behavior under seismic loads in a more practical way. Due to the "pseudo-time" nature of the method, the general behavior of the structure under earthquake loads can be closely monitored during the experiment. In each pseudo time-step, restoring forces are measured by the load cells and the information collected is used with the pre-defined input ground motion, mass and damping properties in order to solve the equation of motion through step-by-step numerical integration. The displacements for the successive steps are calculated and applied to the lateral degrees of freedom of the test structure through servo-controlled hydraulic actuators.

Ground motions used for the pseudo-dynamic tests were synthetic-time acceleration series of the 1999 Düzce earthquake. They were compatible with the site-specific earthquake design spectra for different probabilities of exceedance on different soil types, as shown in **Table 1**. Series of three generated ground

accelerations (named D1, D2, and D3) were imposed on the test specimens subsequently. When compressed in the time domain with a factor of $\sqrt{1/2}$ according to the similitude law, the original ground motions produced the desired earthquake demands on the ½-scaled prototype specimens.

Table 1. Ground Motion Properties

Earthquake GM	Probability of Exceedance (in 50 Years)	Soil Class/Type	PGA/*g*
D1	50%	Z1/Rock	0.254
D2	10%	Z1/Rock	0.545
D3	10%	Z3/Soft Soil	0.604

Forces applied on the specimens were measured by the load cells built in the actuators of the pseudo-dynamic testing system at each story of the test frames. Linear Variable Differential Transformers (LVDTs) were used to measure the story displacements, the 1st and 2nd story column and beam end rotations and joint deformations.

4. TEST RESULTS

Test results of both specimens are presented comparatively in this section. Story displacements, interstory drift ratios, story shear forces and member end rotations are presented, along with selected pictures showing the damages at peak displacements.

The variations of roof displacements with time during the three consecutive ground excitations are shown in **Figure 3**. Roof displacement patterns of the two specimens are quite similar until the highest peak E during D3. Both specimens sustained heavy damage at E, followed by a high residual displacement for SP1 whereas SP2 did not exhibit a significant residual displacement. Difference in column splices does neither explain different residual displacement patterns since the column reinforcement of SP1 was continuous whereas that of SP2 was spliced.

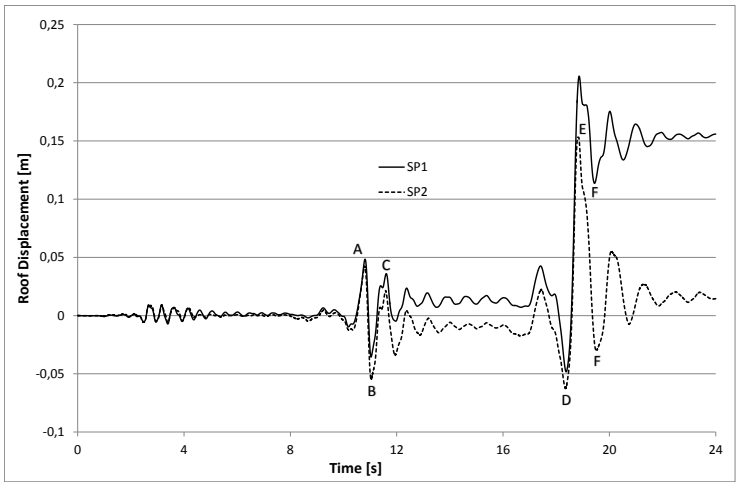

Figure 3. Roof displacement time histories

Damage states of several 1st story members at the six displacement peaks indicated on **Figure 3** are shown in **Figure 4** and **Figure 5** for SP1 and SP2, respectively. The observed damages are fairly similar. Both specimens were in minimum damage state after D1. Minor cracks were observed at the 1st story columns at the peak of D1. Major damages observed during D2 were flexural cracks in both the interior and exterior columns of the 1st story, and the onset of visible cracks in the 1st story joint regions (which initiated prior to cracks in the connecting beam and column ends). Both of these damage formations were directly related to the lack of

confinement at column ends and joint regions. This implies that some inelastic deformations occurred at the 1st story and both specimens were in a moderate damage state after D2. Under D3, the cracks at the bottom ends of the 1st story columns continued to spread and widen. Longitudinal reinforcement pullout phenomenon occurred at the unconfined spliced region of columns in SP2, as shown in **Figure 6**. Damages in the columns were followed by the spread of inclined crack in the joint regions and flexural crack formations at the beam ends. The spread of damage in the upper stories was in the form of shear cracks in the joints and flexural cracks in the upper ends of the 2nd and 3rd story columns. Both frames were in a severe damage state after D3.

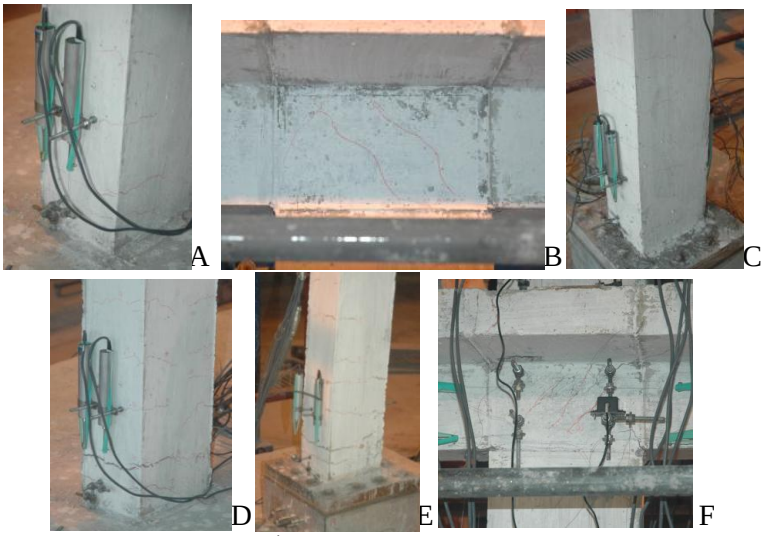

Figure 4. Observed damages at the 1st story members of SP1 at selected displacement peaks

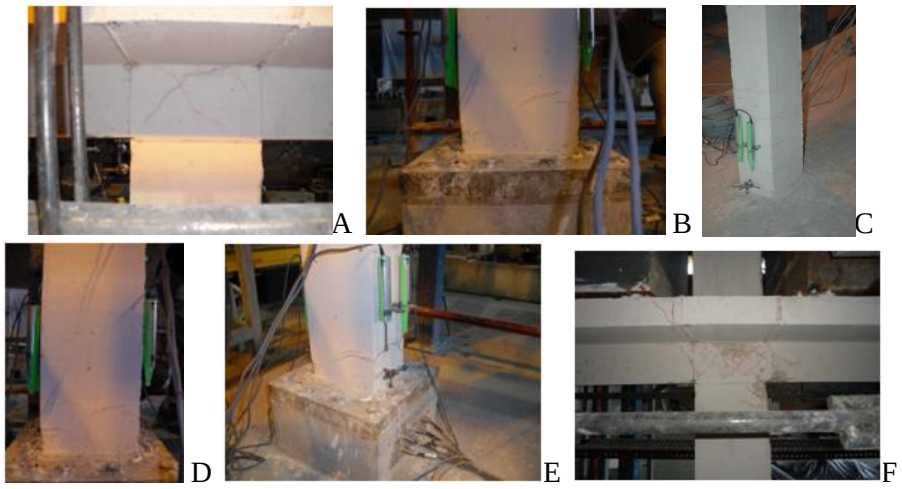

Figure 5. Observed damages at the 1st story members of SP 2 at selected displacement peaks

Figure 6. Reinforcement pullout at the spliced regions of exterior columns (SP2)

1st story interstory drift time histories are presented comparatively in **Figure 7** and maximum recorded values of peak responses are provided in **Table 2**. Base rotations of the 1st story exterior columns and the end rotations of the 1st story beams are also presented comparatively in **Figure 8**. It should be reminded that ideally, the only difference between the two deficient specimens is the presence of insufficient lap splices. However, other inherent factors to consider such as construction methods and material strengths affected the results of the experiments. Thus, these comparisons are presented without detailed discussion as this may lead to misleading interpretations.

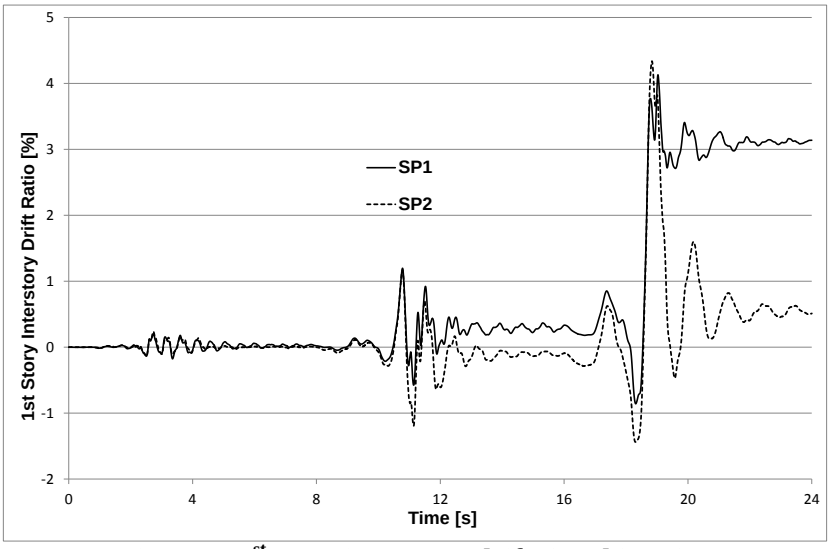

Figure 7. 1st story interstory drift time histories

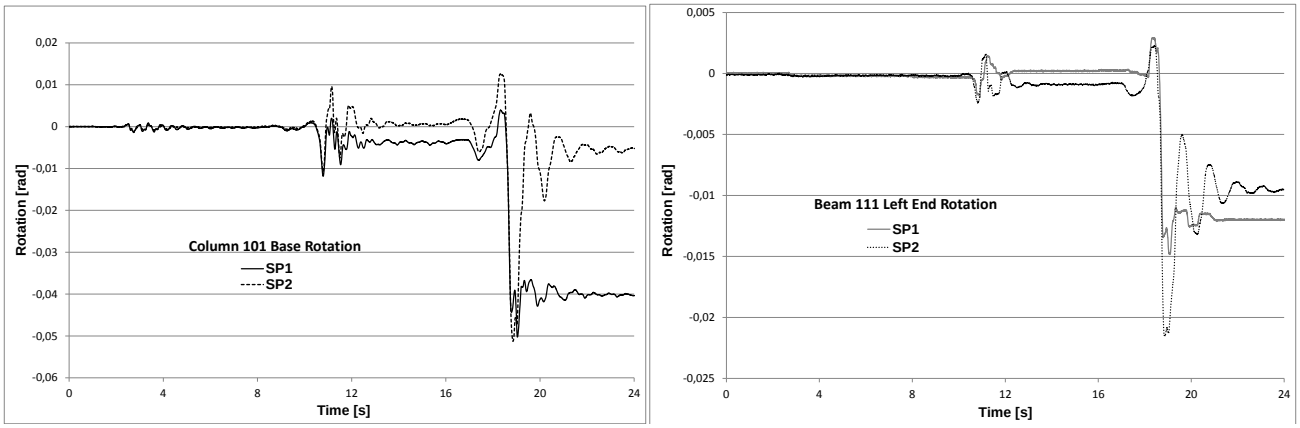

Figure 8. Column 101 (base) and beam 111 (left end) rotation time history comparisons

Table 2. Maximum base shear force, roof displacement, and 1st story drift comparisons

Ground Motion	Max Base Shear *kN*		Max Roof Displacement *mm*		Max 1st Story Drift *%*	
	SP1	SP2	SP1	SP2	SP1	SP2
D1	36.6	38.3	9.4	9.3	0.21	0.24
D2	68.5	71.0	48.7	55.1	1.21	1.19
D3	75.1	67.0	206.0	153.2	4.13	4.34

As far as the interstory drift ratios are considered, both deficient frames are in the minimum global damage state during D1 where maximum interstory drift is less than 0.2%. As the interstory drift ratios reach 1% during D2, frames sustain moderate damage. Finally, they reach heavy damage during D3 at the interstory drift ratios of 4%. Column base rotations in **Figure 8** also follow the same trend with the interstory drift ratios indicating that these two deformation parameters are strongly correlated in deficient frames where columns are weaker than the beams. Beam end rotations in **Figure 8** undergo lower rotations, which is the natural consequence of beams stronger than columns. Apparent joint deformations (**Figure 4** and **Figure 5**) are also influential in lower beam end rotations.

5. PERFORMANCE EVALUATION OF TEST FRAMES ACCORDING TO PERFORMANCE LIMIT STATES OF SEISMIC CODES

Performance levels of the 1st story columns have been assessed in accordance with the strain-based performance limits given in TEC 2007 and the rotation-based performance limits given in ASCE/SEI 41-06. These evaluations were conducted by using the experimental deformation measurements. Selected column member ends were also subjected to careful visual assessments for comparison purposes.

Three similar performance limit states were defined for ductile members according to TEC 2007 and ASCE/SEI 41-06: Immediate Occupancy (IO), Life Safety (LS), and Collapse Prevention (CP). Columns in both specimens satisfy the conditions for pure flexural behavior. The strain limits in TEC 2007 for the longitudinal reinforcement and concrete in compression are presented in **Table 3**, where ρ_s is the volume of existing confining steel and ρsm is the volume of required confining steel. The ρ_s / ρ_{sm} ratio was 0.33 for the columns in both test frames. The plastic rotation limits for columns, which were linearly interpolated for both axial load ratio and shear reinforcement ratio in ASCE/SEI 41-06 (Table 6-8), are also presented in **Table 4**. These performance limits are used to assess the values obtained from the experiments along the plastic hinge length (half of effective section depth), based on the assumption of uniform strain distribution along this region. The performance levels specified in TEC 2007 and ASCE/SEI 41-06 are *minimum damage* (MD) if the measured deformations are less than the IO limits, *significant damage* (SD) if the measured deformations are between IO and LS limits, *heavy damage* (HD) if the measured deformations are between LS and CP limits, and *collapse* (C) if the measured deformations exceed the CP limits.

Table 3. TEC strain based performance limits

Material	Strain Limits		
	IO	LS	CP
Longitudinal reinforcement	0.010	0.040	0.060
Concrete (compression)	0.0035	$0.0035+0.01(\rho_s/\rho_{sm})$	$0.004+0.014(\rho_s/\rho_{sm})$

Table 4. ASCE rotation based performance limits for columns

Column	Plastic Rotation Limits, *rad*		
	IO	LS	CP
Inner	0.0043	0.0101	0.0120
Outer	0.0048	0.0117	0.0140

The measured performance levels for each specimen are also compared with the observed damages from the pseudo-dynamic tests. The observed damages were assessed as objectively as possible, as the goal of these evaluations is to compare the performance predictions of TEC 2007 and ASCE/SEI 41-06 with the physical damages observed in the laboratory. Performance evaluations strictly focus on the D2 ground motion because D1 is too weak and D3 brings the system to collapse.

Table 5 compares the performance levels at the 1st story column member ends during D2 based on the recorded test values and the observations from SP1. During ground motion D2 in the physical test, flexural

macro-cracks were visible at the 1st story column bottom ends (see **Figure 4**A) which indicate that inelastic deformations occurred in the columns. Hence all 1st story column bottom ends in the experiment after D2 were considered in the SD performance level whereas the top ends being in the MD performance level. Both ASCE/SEI 41 and TEC seem to capture the observed performances perfectly well. Concrete compressive strains govern the TEC evaluation, which are given for column bases in **Table 5**. The corresponding values for the plastic rotations are also given in the same table, along with the yield rotations. These figures indicate a rotation ductility of 1.5 for the deficient column bases which are in good conformance with the observed damages. It should be noted from **Table 4** however that the recorded plastic rotations are very close to the LS limits of ASCE/SEI 41 although the rotation ductility was very low. Acun and Sucuoğlu10 also noted the conservatism of ASCE/SEI 41 rotation limits for deficient concrete columns.

Table 5. 1st story column performance levels of SP1

Performance assessment procedure	Column 101		Column 102		Column 103		Column 104	
	Bot.	Top	Bot.	Top	Bot.	Top	Bot.	Top
EXP (TEC) ε_c	SD 0.0056	MD	SD 0.0064	MD	SD 0.0054	MD	SD 0.0052	MD
EXP (ASCE) θ_p θ_y	SD 0.0103 0.0191	MD	SD 0.0101 0.0190	MD	SD 0.0101 0.0190	MD	SD 0.0073 0.0191	MD
Observation	SD	MD	SD	MD	SD	SD	SD	MD

Performance levels at the 1st story column ends after D2 are compared in **Table 6** for SP2. Visual observations on the columns after D2 have indicated very similar column damages with SP1 (see **Figure 4**C and **Figure 5**C). Flexural cracks were observed, but there was no crushing of concrete cover and there was almost no permanent drift. Reinforcement pullout was not observed during D2. Therefore all columns in SP1 after D2 can be declared in the same performance level as of the SP1 columns. TEC predicted the observed column performances exactly, but ASCE/SEI 41 predicted three of the four column ends in the collapse (C) performance level. This is due to the fact that ASCE/SEI 41 has no tolerance for columns which have lap splice deficiencies. Once the member end rotates past the yield value, it is immediately classified as being in the collapse performance level. Therefore ASCE/SEI 41 rotation-based assessment is overly conservative in this regard, as the physical specimen was still in relatively good condition after this ground motion.

Table 6. 1st story column performance levels of SP2

Performance assessment procedure	Column 101		Column 102		Column 103		Column 104	
	Bot.	Top	Bot.	Top	Bot.	Top	Bot.	Top
EXP (TEC) ε_c	SD 0.0061	MD	SD 0.0063	MD	SD 0.0064	MD	SD 0.0049	MD
EXP (ASCE) θ_p θ_y	C 0.0094 0.0191	MD	C 0.0089 0.0190	MD	C 0.0092 0.0190	MD	C 0.0068 0.0191	MD
Observation	SD	MD	SD	MD	SD	MD	SD	MD

6. ANALYTICAL MODELING

The OpenSees Simulation Platform was used for generating the models (referred to as OS in Tables and Figures) of each specimen in order to estimate the seismic response of the test frames. Beams and columns were modeled by using the force-based elements defined with nonlinear fibre sections at integration points. Second order geometric nonlinearity effects were considered in columns. Formulation of the *Nonlinear Beam Column Element* follows the Euler-Bernoulli beam theory, which ignores shear deformations. For the joint regions, joint offsets

were made at the element ends for both beam and column elements in accordance with the procedures defined in ASCE/SEI 41-06. Most column rigid end zones were taken as zero in order to compensate for the effect of joint rotation on column stiffness as this system was a strong beam-weak column system. Beam lengths were defined from centerline to centerline of the adjacent columns. Shear deformations at the beam-column connection regions were neglected in the frame models.

The concrete material model used in the OpenSees models was *Concrete01*, which is the uniaxial Kent and Park concrete material model with no tensile strength and degraded linear unloading/reloading stiffness as proposed by Karsan and Jirsa. Through this material model, confinement effects of transverse reinforcement were accounted for by increasing the strength and strain capacities of the unconfined concrete in order to reflect the behavior of concrete in the confined zones, which have a residual stress associated with them. A stress-strain relation was defined using the *uniaxialMaterial ReinforcingSteel* command with 90% of the yield and ultimate strength values of the reinforcing steel obtained from material tests, to provide more realistic predictions of column strengths. An onset strain hardening value of 0.01 and an ultimate strain value of 0.1 was used, as suggested by TEC 2007. The *ReinforcingSteel* material model was created specifically for simulating reinforcing steel in a fiber section. A perfect bond between the concrete and steel was assumed in the models.

Dynamic properties of the specimens were modeled as lumped masses at the nodes with Rayleigh damping assumed for the time history analyses. The damping value was set at 2.5% for stability purposes in the PsD testing. The *Dynamic Ground-Motion* analysis feature in OpenSees was used to simulate the frame's nonlinear dynamic response to the ground motions. The Krylov-Newton time-stepping algorithm was used to better capture strength degradations. The force-based beam and column elements had 5 Gauss-Lobotto integration points.

The results from the experiments and the analytical models are compared for two global parameters (roof displacements and base shears) and one local parameter (interstory drift ratios) in order to test the success of analytical models in predicting inelastic dynamic response.

6.1. Test Frame SP1

Roof displacement and base shear force variations with time are shown in **Figure 9**. The errors in the peak roof displacements are 24, 16 and 15 % during D1, D2 and D3 whereas the similar errors in base shear are 13, 2 and 11 %, respectively. The model performs quite well in predicting the residual displacement which is always a challenge. Nevertheless, the under estimation error is 42%. When the 1st story interstory drift ratios are compared in **Figure 10**, errors grow up. They are 80, 37 and 50% at the peaks of D1, D2 and D3, respectively. This is more or less the same for the stories above.

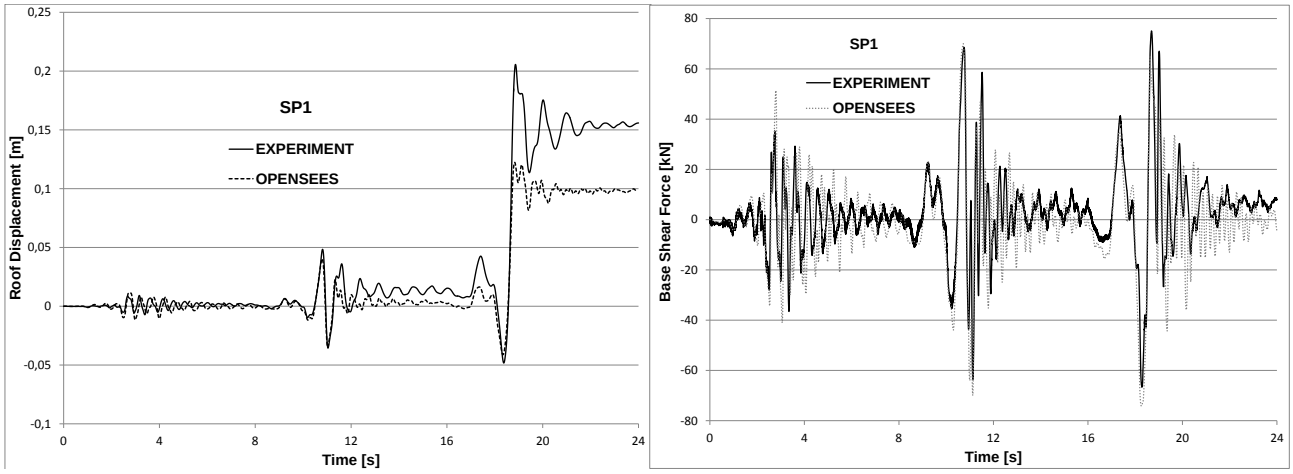

Figure 9. Base shear force time history comparison (SP1)

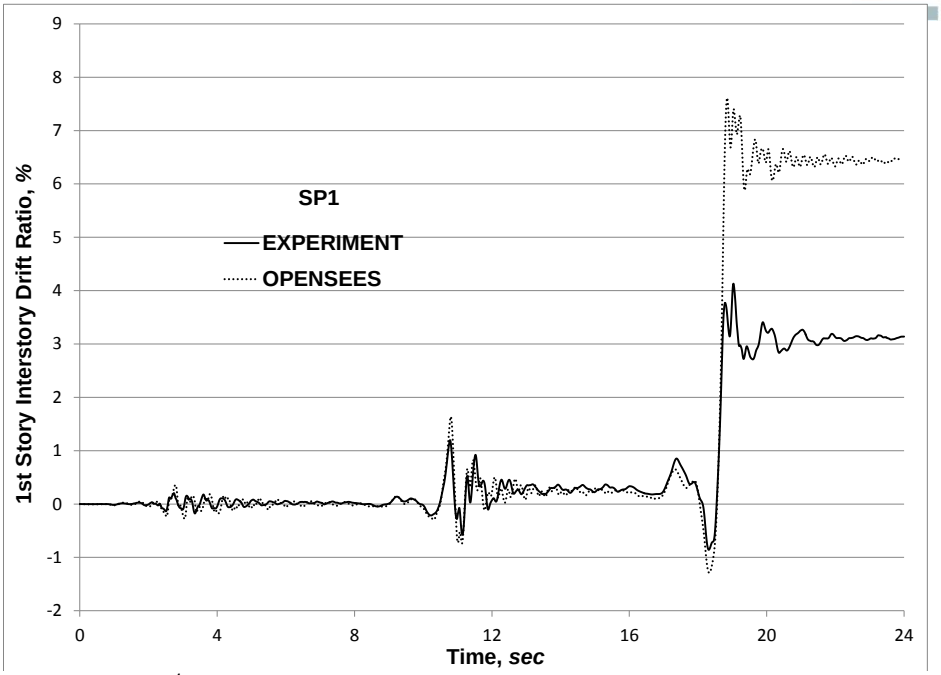

Figure 10. 1st story interstory drift ratio time history comparison (SP1)

6.2. Test Frame SP2

Since this specimen had lap splices, separate elements were created in the spliced regions. The splice lengths do not conform to the $40d_b$ length as required by TEC 2007 (only 75% of this length was provided). To account for this deficiency, the yield strength reduction in the model for these spliced-region elements were reduced linearly, as suggested by TEC 2007 and exponentially, as suggested by ASCE/SEI 41-06.

The roof displacement and base shear force variations with time are shown in **Figure 11**. The 1st story interstory drift ratio time history comparison is shown in **Figure 12**. The model results for two different lap splice yield strength reductions are almost the same. The errors in the peak roof displacements are 19, 25 and 35 % during D1, D2 and D3 whereas the similar errors in base shear are 41, 10 and 21 %, respectively. These are larger than the errors for SP1. The model gives the same residual displacement for SP1, however the residual displacements of SP2 were much less. The errors in the 1st story interstory drift ratios are 50, 46 and 4% at the peaks of D1, D2 and D3, respectively.

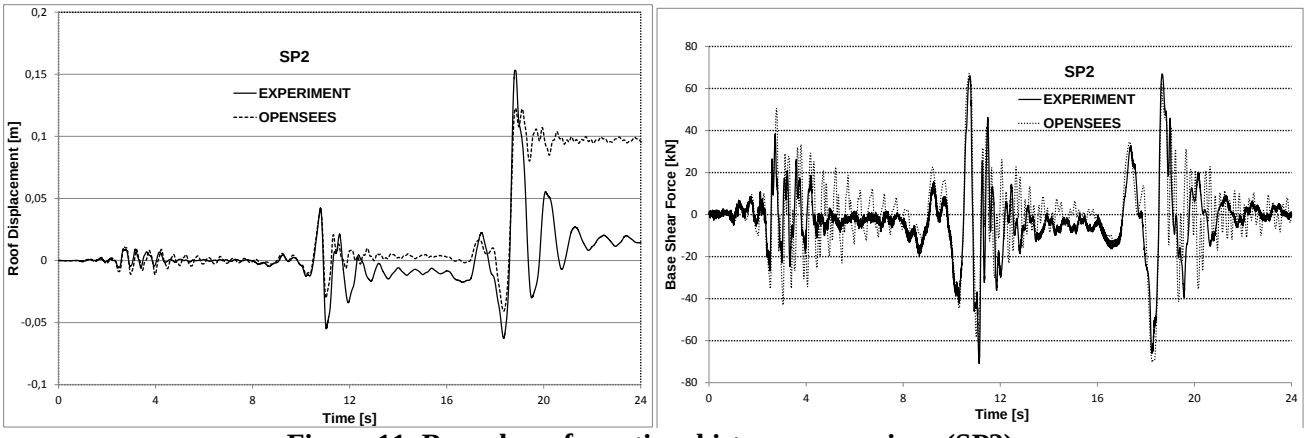

Figure 11. Base shear force time history comparison (SP2)

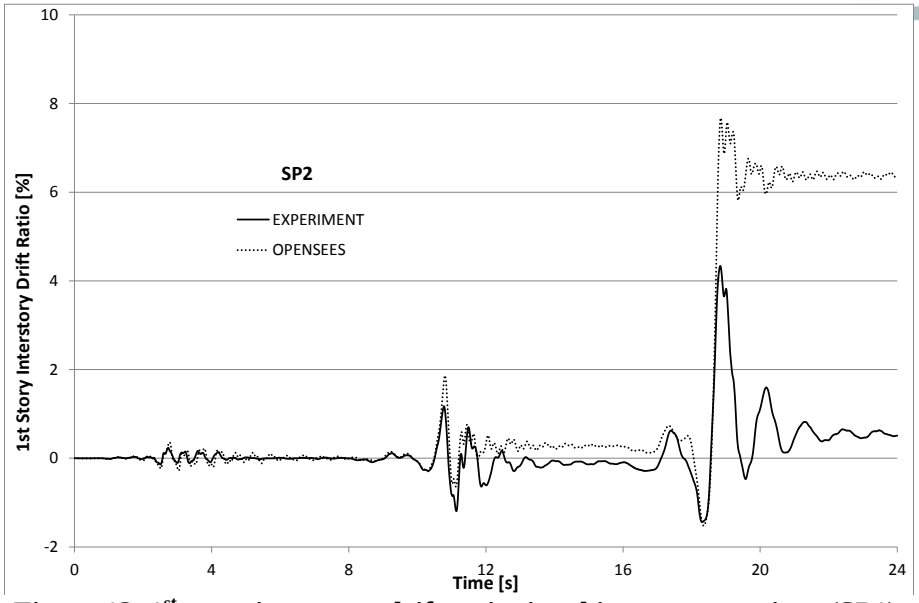

Figure 12. 1st story interstory drift ratio time history comparison (SP1)

Although very rigorous analytical models have been developed for SP1 and SP2, the errors in the global and local response parameters are significant. This is questioning the validity of performance assessment procedures in performance-based seismic codes for predicting the seismic performance of "deficient concrete frames". The situation becomes even more complicated when non-structural components interact with structural components during dynamic response.

7. SUMMARY AND CONCLUSIONS

Results of pseudo-dynamic tests on two 3-story, 3-bay deficient concrete frames are presented in this study. Numerical models in OpenSees were developed in order to simulate the results of the pseudo-dynamics tests. Global and local responses predicted by these models were examined and performance evaluations were conducted according to nonlinear procedures in TEC 2007 and ASCE/SEI 41-06.

Specific to the specimen with lap splice deficiencies, the lack of tolerance beyond the yield rotation experienced by a column as defined in ASCE/SEI 41-06 lead to overly conservative results. Damages observed did not justify the classification of member ends to be in such extreme performance level. A 25% lap splice length deficiency did not seem to be as detrimental to the specimen as what ASCE/SEI 41-06 assessment estimated them to be. Furthermore, the presence of 25% deficient lap splice lengths in the laboratory for the second specimen did not affect the overall response, or change the failure mode when compared to the first specimen. Therefore, code requirements for lap splice lengths can be seen as quite conservative and are able to tolerate deficiencies up to 25% of the required length.

Modeling materials in deficient systems by using nominal but reduced strength properties in hopes to predict accurate seismic responses was not very efficient in the OpenSees models. The main cause was the inability of modeling degradation during the ground motions. Furthermore, unless joint deformations are explicitly accounted for, local deformations such as end rotations cannot be captured. In general, estimating seismic responses of deficient concrete frames is an extremely challenging, if not impossible, task.

ACKNOWLEDGEMENT

This study was conducted with the financial support provided by the Turkish Scientific and Technological Research Council (TUBITAK) with the Grant No: 108G034.

REFERENCES

Aboutaha, R.S., Engelhardt, M.D., Jirsa, J.O. and Kreger, M.E. (1996). Retrofit of Concrete Columns with Inadequate Lap Splices by the Use of Rectangular Steel Jackets. *Earthquake Spectra* **Vol. 12**, **No. 4**, 693-714.

Acun B. and Sucuoğlu, H. (2010). Performance of Flexure Controlled Concrete Columns under Severe Displacement Cycles. *ACI Structural Journal* **Vol. 107**, **No. 3**, 364-371.

ASCE/SEI 41 (2007). Seismic Rehabilitation of Existing Buildings, American Society of Civil Engineers, Reston, VA.

Canbay, E., Ersoy, U. and Özcebe, G. (2003). Contribution of Reinforced Concrete Infills to Seismic Behavior of Structural Systems. *ACI Structural Journal* **Vol. 100**, **No. 5**, 637-643.

Comite Europeen de Normalisation (2005). European Standard EN 1998-3 Eurocode 8: Design of Structures for Earthquake Resistance – Part 3: Assessment and Retrofitting of Buildings, Brussels.

Eshghi, S. and Zanjanizadeh, V. (2008). Cyclic Behavior of Slender R/C Columns with Insufficient Lap Splice Length. *14th World Conference on Earthquake Engineering*, Beijing, China.

Karsan, I.D., and Jirsa, J.O. (1969). Behavior of Concrete under Compressive Loading. *Journal of Structural Division*, ASCE **Vol. 95**, **No. ST12**, 2543-2563.

Kent, D. C. and Park R. (1971). Flexural Members with Confined Concrete. *Journal of Structural Division*, ASCE **Vol. 97**, **No. ST7**, 1969-1990.

Lynn, A. C., Moehle, J. P., Mahin, S. A., and Holmes, W. T. (1996). Seismic Evaluation of Existing Reinforced Concrete Building Columns. *Earthquake Spectra* **Vol. 12**, **No. 4**, 715-739.

Melek, M. and Wallace, J.W. (2004). Cyclic Behavior of Columns with Short Lap Splices. *ACI Structural Journal* **Vol. 101**, **No. 6**, 802-811.

Ministry of Public Works and Settlement (2007). Turkish Earthquake Code: Specifications for Buildings Constructed in Disaster Areas, Ankara.

OpenSees (2011). Open System for Earthquake Engineering Simulation. Available from: http://opensees.berkeley.edu.

Takanashi, K., Udagawa, K., Seki, M., Okada, T., and Tanaka H (1975). Nonlinear earthquake response analysis of structures by a computer-actuator on-line system. *Bulletin of Earthquake Resistant Structure Research Center 8, Institute of Industrial Science*, University of Tokyo, Japan.